

Ultrafast reflectometry on the RFX-mod device

G. De Masi, R. Cavazzana, M. Moresco, E. Martines

Consorzio RFX, Euratom-ENEA Association, Corso Stati Uniti 4, I-35127 Padova, Italy

1.Introduction. It is well known that reflectometric measurements can be seriously disturbed by the presence of a high level of plasma density fluctuations, because of its deleterious effect on the wave scattering¹. In this sense the Reversed Field Pinches, as RFX-mod², represent a very challenging test-bed since their edge properties are characterized by a wide spectrum of density fluctuations. Moreover, the presence of a so called *reversal region* at the edge in which the toroidal component, B_ϕ , of the magnetic field reverses, leads to some crucial implications: the poloidal component, B_θ , becomes the main one, and a strong toroidal flow (up to ten times larger than in a tokamak) builds as effect of the interaction with the radial electric field E_r ; all of the $m=0$ MHD modes resonate due to the presence of a $q=0$ surface, creating a chain of poloidally symmetric islands in the outer plasma (see Fig. 1, obtained with a Field Line Tracing code³). Recently, operating at high plasma current I_p , this frame became even richer, with the appearance of the so called *quasi single helicity* (QSH) states, in which the plasma gets globally self-organized in a helical rotating geometry ($m=1, n=-7$), associated to a considerable improvement of the confinement properties⁴. In this complex scenario the traditional and widely used reflectometric schemes to detect the plasma position can result inefficient¹. In this contribution we present the main features of the new concept RFX-mod microwave reflectometer and we show and discuss the most significant results since last year.

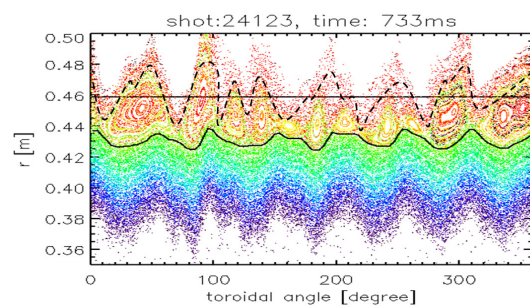


Fig.1: Poincaré plot in the (r, ϕ) plane of the outer region of RFX-mod (the horizontal line marks the position of the first wall). The local displacement $\delta_{m=1}$ (continuous line) and $\delta_{m=0}$ (dashed line) are overlotted (see sect. 3).

2.Experimental setup. The RFX microwave reflectometer system was originally designed with 5 bands⁵ covering a frequency range between 26.5 GHz and 110 GHz, already with the idea to overcome the aforementioned issues characterizing the RFP configurations such as the high level of density fluctuations and the high magnetic shear. Nevertheless, a further analysis¹ highlighted the need for a successive upgrade. With the help of a simplified two-dimensional model mimicking the dynamics of the plasma turbulence and the frequency sweep, the basic mechanisms that critically affect the measurements have been outlined. It turned out that a bidirectional frequency sweep with an adequate modulation rate can make

the reflectometric signal able to endure the effect of the small scale density fluctuations coupled at the edge with the toroidal flow.

Keeping these considerations in mind, the first upgraded Ka-band (27-30 GHz), composed by an IMPATT oscillator microwave source and driven with an *ultrafast* modulation rate (4 GHz/ μ s) has been installed on the RFX-mod device since last year, after a preliminary source calibration phase⁶ to obtain the time-frequency characteristic curve. Thanks to this new scheme, the radial position $d(t)$ of the cut-off layer ($1-1.2 \times 10^{19} \text{ m}^{-3}$) can be evaluated¹ from the measured group delay τ_g with a very high time resolution (1 μ s) as:

$$\langle \tau_g \rangle_{t_1}^{t_2} = \frac{1}{2\pi} \left\langle \frac{D\phi(t)}{Dt} \right\rangle_{t_1}^{t_2} = 2 \frac{2\pi}{c} \left[\alpha \langle d(t) \rangle_{t_1}^{t_2} + F_0 v_{rad} \right],$$

where $\Phi(t)$ is the *phase delay* introduced by the scattering with the plasma (whose algebraic form can take into account different density profiles), α is the sweep rate (Hz/s), F_0 is the center sweep frequency, t_1 and t_2 are the time intervals corresponding to the ascending and descending frequency sweeps and v_{rad} is the plasma radial velocity (Doppler effect). The latter term, caused by the long wavelength density fluctuations, giving the same contribution on both ascending and descending frequency sweep, can be cancelled by analyzing the difference of the two beat signals¹ and the group delay can be correctly recovered.

3.Experimental results and discussion. In this section we present the first reflectometric measurements analyzed in the light of the aforementioned model. Fig. 2 shows a typical time

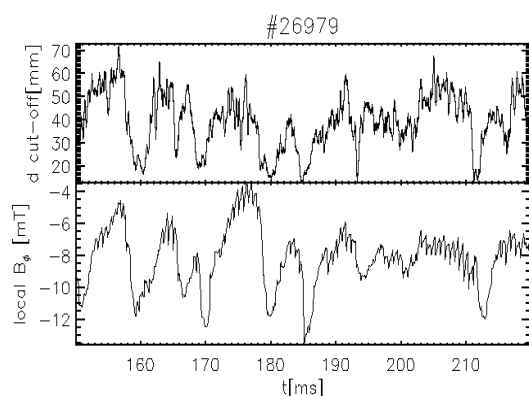


Fig.2: Top: time evolution of the cut-off layer. Bottom: time evolution of the local B_ϕ .

evolution of the cut-off density layer ($1-1.2 \times 10^{19} \text{ m}^{-3}$) for the Ka-band, over an high plasma current ($I_p > 1 \text{ MA}$) discharge flat-top phase. A preliminary work⁶ concerned the *validation* of such a new measurement concept through the comparison with the interferometric measurements and the Thermal Helium Beam diagnostics⁷. Then we moved to a more local analysis oriented to highlight the role of the edge

magnetic field in determining the radial position of the cut-off layer. Fig. 2 reveals, in particular, a clean correlation with the fluctuations of the local toroidal component, B_ϕ , of the magnetic field. This first result suggests a relation between the edge density and the local magnetic topology, characterized in the customary high plasma current RFX-mod operations by the superposition of the $m=0$ islands at the edge and of the more internal QSH

deformation. Furthermore, being the radial position of these islands defined by the value of the reversal parameter F (defined as $B_\phi(a)/\langle B_\phi \rangle$), during the *shallow* F discharges ($F > -0.07$), most of $m=0$ islands are pushed outwards, and the related field lines intercept the first wall before closing again⁸. This leads at the edge to a quite complex frame, as shown in Fig. 1. In the same figure, the local displacements ($\delta_{m=0}$, $\delta_{m=1}$) respectively due to the $m=0$ and the $m=1$ deformations are separately plotted and represent a more compact way to figure the edge magnetic topology⁹. More in detail, they allow us to compare the time evolution of the magnetic dynamics at a fixed toroidal position with the radial position of cut-off layer as evaluated from the reflectometer (Fig. 3). From these measurements the local evolution of the cut-off layer at the edge appears to be dominated by the local QSH helical modulation $\delta_{m=1}(t)$ when the $m=0$

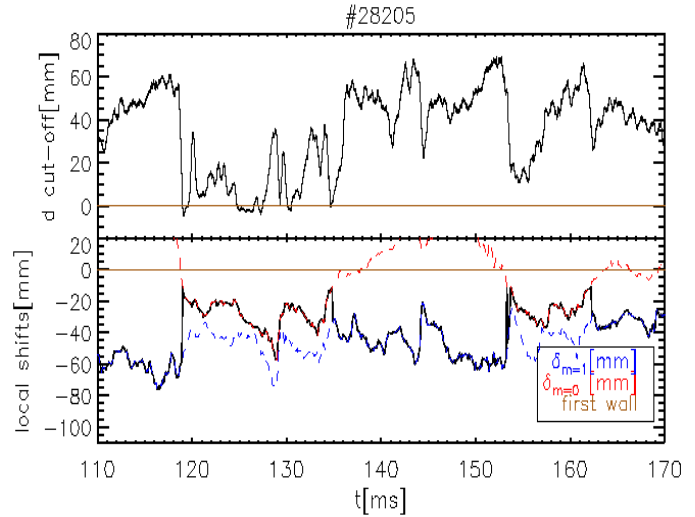


Fig.3: *Top*: time evolution of the cut-off layer. *Bottom*: the black line is alternatively built by tracing the $m=0$ deformation (if $\delta_{m=0} < 0$) or the $m=1$ one (if $\delta_{m=0} \geq 0$).

islands intercept the first wall ($\delta_{m=0}(t) > 0$), while these islands seems to play an important role only when their field lines locally close into the chamber ($\delta_{m=0}(t) < 0$).

In the light of these results we moved our attention to the average behaviour on a shot to shot basis during the QSH states, in order to understand what are the mechanisms that regulate the local plasma-wall interaction. In Fig.4 a clear trend of the radial position of the cut-off layer is

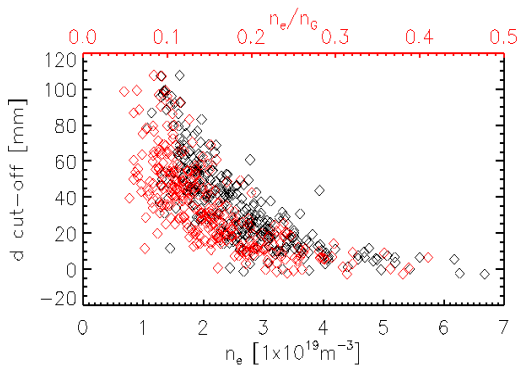


Fig. 4: Scaling plot of $\langle d \text{ cut-off} \rangle$ vs n_e (black diamonds) and n_e/n_G (red diamonds).

recognizable as a function of both the global electron density n_e and of the parameter n_e/n_G (the electron density normalized to the Greenwald one). In both cases the distance of the plasma from the antenna decreases by increasing n_e or n_e/n_G , showing, in particular, a saturation when $n_e/n_G \geq 0.3$. This limit is consistent with some previous results^{10,11} obtained on the RFX-mod device. Due to this crucial role of the global

density, we performed a similar analysis (Fig. 5), by averaging over a shots database at different plasma currents I_p but with comparable electron density n_e ($[2.7\text{-}3.2] \times 10^{19} \text{ m}^{-3}$) and

F values ($[-0.02,-0.05]$). Also in this case a clear trend is recognizable, highlighting a smaller and smaller local interaction with the first wall by increasing the plasma current. Finally, keeping almost constant density and plasma current ($[1,1.2]$ MA), we were able to isolate the contribution due to the value of the reversal parameter F . In fact, in Fig. 5 a relatively important dependence of the radial position of the cut-off layer on the F value is shown passing from a shallow configuration ($F > -0.07$) to a deep configuration ($F < -0.1$). These two last results deserve a further deepening, since, even if they figure only a local picture of the edge plasma behaviour, they could partially explain the reason why the improved RFX-mod regimes, such as QSH states, appear much more frequently by increasing plasma current and operating at shallow F configuration⁵. Moreover, looking at Fig. 5 along with Fig. 3 the interplay of the $m=1$ and the $m=0$ local deformations could justify the change in the regime observed in the average behaviour at different F values (linked to the position of the islands).

4.Conclusion. From a technical point of view the ultrafast microwave reflectometry turned out to be a very reliable tool for the edge density monitoring. In particular, the capability to operate in adverse conditions (such as the presence of a high level of density fluctuations), having as a unique demand to adapt the working frequency range to the edge electron density, together with an easy possible development towards a real-time measurement, makes this diagnostics suitable for a reactor application. From a physical point of view, the results here presented highlight the main features of the edge density dynamics on the RFX-mod device. In particular, they suggest a relation with the local magnetic topology that cannot be set aside in order to understand which are the key parameters regulating the local plasma-wall interaction. Nevertheless, to extend this interpretation to a global edge picture, a direct check with other diagnostics monitoring the outer region of the RFX-mod would be strongly needed.

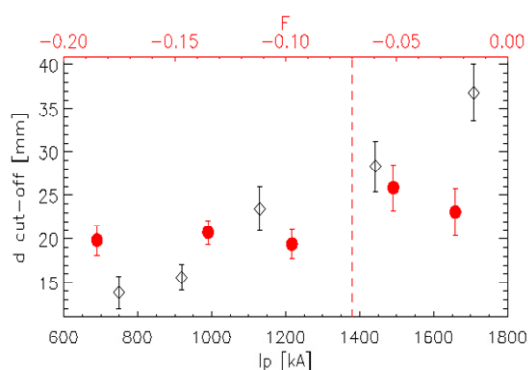


Fig. 5: Scaling plot of $\langle d \text{ cut-off} \rangle$ vs I_p (black diamonds and axis) and F (red symbols and axis)

This work was supported by the European Communities under the contract of Association between EURATOM/ENEA. The views and opinions expressed herein do not necessarily reflect those of European Commission.

References

- ¹ R. Cavazzana et al., Rev.Sci.Instrum., **79** 10F105 (2008)
- ² P. Sonato et al., Fusion Eng.Des., **161**, 66-68 (2003)
- ³ P. Innocente et al., Nucl.Fusion, **47**, 1092 (2007)
- ⁴ R. Lorenzini et al., Nature Phys., **5**, 570 (2009)
- ⁵ M. Moresco et al., IJIMW, **12**, 609 (1992)
- ⁶ G. De Masi et al., 1st ICFDT, Frascati ,25-27/11 (2009)
- ⁷ M. Agostini et al., PPCF, **51**, 1050003 (2009)
- ⁸ E. Martines et al., Nucl.Fusion, **50**, 035014 (2010)
- ⁹ P. Zanca and D. Terranova, PPCF, **46**, 1115 (2004)
- ¹⁰ P. Scarin et al., J.Nucl.Mater.,**390-391**, 444-447 (2009)
- ¹¹ M. E. Puiatti et al., PoP, **16**, 012505, (2009)